CAMBRIDGE
Cambridge University Press
978-1-107-40851-7 - Actinides 2008—Basic Science, Applications and Technology: Materials Research Society Symposium Proceedings: Volume 1104
Editors: David K. Shuh, Brandon W. Chung, Thomas Albrecht-Schmitt, Thomas Gouder and Joe D. Thompson
Excerpt
More information

Phase Transformation and Metallurgy

Mater. Res. Soc. Symp. Proc. Vol. 1104 © 2008 Materials Research Society 1104-NN01-02

Electronic Phase Transitions in *f*-electron Metals at High Pressures: Synchotron X-ray Spectroscopic Studies on Gd to 100 GPa

Choong-Shik Yoo[1], Brian Maddox[2], and Valentin Iota[2]
[1]Department of Chemistry and Institute for Shock Physics, Washington State University, Pullman, WA, 99164
[2]Lawrence Livermore National Laboratory, Livermore, CA, 94551

ABSTRACT

Unusual phase transitions driven by electron correlation effects occur in many *f*-electron metals (lanthanides and actinides alike) from localized phases to itinerant phases at high pressures. The dramatic changes in atomic volumes and crystal structures associated with some of these transitions signify equally important changes in the underlying electronic structure of these correlated *f*-electron metals. Yet, the relationships among the crystal structure, electronic correlation and electronic structure in *f*-electron metals have not been well understood. In this study, utilizing recent advances in third-generation synchrotron x-ray spectroscopies and high-pressure diamond-anvil cell technologies, we describe the pressure-induced spectral changes across the volume collapse transition in Gd at 60 GPa and well above. The spectral results suggest that the *f*-electrons of high-pressure Gd phases are highly correlated even at 100 GPa – consistent with the Kondo volume collapse model and the recent experimental evidence of strong electron correlation of α-Ce.

INTRODUCTION

The *f*-electron metals, actinides and lanthanides alike, exhibit a profound change in character, both for individual metals as a function of compression, or across the series as a whole at ambient pressure, as illustrated in Fig. 1 [1]. The early part, from Th-Pu, shows a parabolic behavior of the equilibrium molar volume reminiscent of the *d*-transition metals, whereas the later part shows a more constant behavior of the specific volume as a function of atomic number. The similarity between the light actinides and the d-transition metals in this regard is governed by the fact that the light actinides and the *d*-transition metals both have delocalized electrons, *f* and *d* respectively. For the heavier actinides

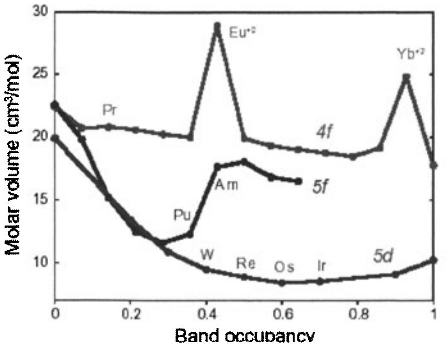

Figure 1. *Specific volumes of f- and d-electron transition metals plotted as a function of their band actinides occupancy. Divalent Eu and Yb are the exceptions to the systematic behavior of other trivalent rare-earth metals.*

from americium and on, however, the *5f* electrons are localized similar to the lanthanide series and their properties become quite different from that of the earlier actinides.

Plutonium, at the central position of the two trends, exhibits a dramatic effect with a subtle change in lattice induced by pressure, temperature and impurities [2]. For example, Pu at ambient conditions crystallizes into low symmetry monoclinic α-Pu with 16 atoms per unit cell suggesting itinerant electrons participating in bonding, whereas at slightly elevated temperatures it undergoes a series of phase transitions to high symmetry *fcc* δ-Pu with localized *5f* electrons. Because of this fundamental difference in *5f*-electron correlation/bonding, these two phases of α- and δ-Pu have very different thermodynamic, mechanical and chemical properties including a huge difference in density near 20 %. The dramatic changes in atomic volumes and crystal structures associated with some of these transitions signify equally important changes in the underlying electronic structure of these correlated *f*-electron metals. The evidences include a very complicated phase diagram of Plutonium with seven polymorphs at the ambient pressure alone and several more at high pressures and a highly unusual minimum in the melt curve.

Analogous to the δ–α phase transition of Pu, rare-earth metals also exhibit unusual electronic phase transitions at high pressures. Figure 2 summarizes the pressure-induced structural phase transitions in the early trivalent rare-earth metals, from high-symmetry closed-packed structures (colored in red) at low pressures to low-symmetry complex structures (in blue) at high pressures [1]. Similarly, these transitions are considered to occur as a result of the pressure-induced *4f*-valence electron delocalization, but its exact nature is not well understood. For example, some of these transitions are accompanied with large volume collapse (for example, 15 % in Ce at 1 GPa, 10 % in Pr at 20 GPa and 5 % in Gd at 60 GPa), yet the others like Nd and Sm transform to itinerant phases without any apparent discontinuity in volume. No collapse has been found in the late series of rare-earth metals. It is not known if there exist similar volume collapse transitions in Nd and Sm at low temperatures or at higher pressures than we have studied to date. Neither is known if such a large volume collapse is a direct manifestation of any abrupt electronic structure change.

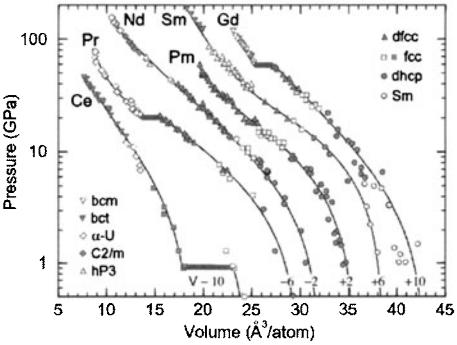

Figure 2. *Unusual electronic phase transitions of the early rare-earth metals from high-symmetry closed-packed structures of correlated phases (in red symbols) at low pressures to low-symmetry complex structures of itinerant phases (in blue) at high pressures.*

Generally speaking, the effects of electron correlation diminish with pressure as shown in Fig. 2, yet the underlying physical mechanism is not established- neither experimentally nor theoretically. There are two emerging conjectures for the origin of the volume collapse. One is a "Mott transition" in which high pressure causes an increased overlap between initially localized *f*-electron orbitals and a resulting change to a metallic phase [3]. This band widening also causes the destruction of local magnetic moments. This transition occurs abruptly in a first-order, which may end at a critical point at high temperatures. The competing "Kondo volume collapse" mechanism suggests instead that the important pressure-induced change is in the localized-valence electron coupling [4,5]. In such, the local moment of *f*-electrons is only screened by the valence- and/or their own *f*-electrons- not quenched. This transition is then expected to occur more continuously with increasing pressure. An abrupt reduction in volume may or may not occur at a critical level of such electron screening. As a result, no theory has yet been able to convincingly explain the existence (or absence) of such a volume collapse, nor simultaneously describe both of the phases that lie to either side of the electronic volume-collapse transition.

Despite the apparent relationship between crystal and electronic structures in *f*-electron metals, the high-pressure experiments to date have been focused largely on probing crystal structural properties. There are little data regarding the electronic structures of phases at high pressures. Clearly, the combined information of electronic spectral data and crystal structural data is critical to discriminate between different underlying mechanisms proposed to explain these unusual electron correlation-driven, structural phase transitions and, thus, to gain insight into these unusual electronic phase transitions. This is exactly an overarching goal of the present study, and in this paper we highlight the spectral changes observed in Gd to 100 GPa [6].

EXPERIMENTAL RESULTS

Probing *f*-electronic states in actinide and lanthanide metals at high pressures is, however, challenging, because the governing electronic states are located at relatively low energies. For example, the M-edges are less than 1 keV, and the *f*-electron states are within only a few eV apart from the Fermi level. Theoretical expectations are that the *f*-electron density of states should be "Hubbard split" by ~ 6 and ~ 4 eV for the rare-earths and actinides respectively, whereas in the itinerant phases this splitting is absent and the *f*-density of states should be a contiguous structure overlapping the Fermi level [1]. High-pressure investigations of such low energy transitions are not feasible using a conventional x-ray absorption technique, because of strong x-ray absorption by diamond and/or any metal gasket. In fact, such soft x-rays do not even penetrate through the bulk of *f*-electron metal samples and, thus, the studies have been focused on probing the *f*-electron states largely on the surface and at the ambient pressure.

High intensity, third-generation x-ray offers new ways to investigate relatively low-energy electronic states from the bulk at high pressures, by using relatively high-energy x-ray with high energy resolution, $\Delta E/E > 10^4$. Furthermore, combining with recent developments of radial x-ray DAC technologies utilizing high-strength x-ray translucent Be gaskets (in the spectral region of 5-10 keV, otherwise blocked by strong diamond absorption), it is now possible to utilize a variety of high-resolution x-ray spectroscopic methods to probe the pressure-induced changes in electronic transitions, *f/d* (or, valence)-electron hybridization, and local moments in *f*-electron metals, all at 100 GPa pressures.

Over the past several years, we have developed/applied a wide array of x-ray spectroscopic methods to probe electronic and magnetic properties of *3d/4f*-electron metals in diamond anvil cells at pressures to 100 GPa. The spectroscopic methods used include x-ray absorption spectroscopy (XAS), resonant inelastic x-ray scattering (RIXS), x-ray emission spectroscopy (XES), and x-ray circular dichroism (XMCD) [6-9]. Many of these experiments have been performed at the HPCAT beamline (16IDD) of the APS. Among these results, in this paper we summarize the XAS, RIXS, and XES data of Gd, all obtained at high pressures to 100 GPa well above the volume collapse transition at ~60 GPa, so as to understand the exact nature of electronic correlation in highly compressed Gd.

A. L-edge X-ray Absorption Spectroscopy (XAS)

X-ray absorption spectra with high energy resolutions are typically composed of two distinctive features; (i) x-ray absorption near edge structure (XANES), covering the region between a few eV below the binding energy E_o (often called as a pre-edge) and ~10 eV above the E_o (a near edge) and arising from electron excitations from core levels to higher unfilled, half-filled orbitals, or non-bound levels, and (ii) near/extended edge x-ray absorption fine structure (N/EXAFS), covering the region above 10 eV and arising from scattering processes of the ejected photoelectrons by the coordinating shells and neighboring atoms. Therefore, the XANES probes the electronic density of state of unoccupied final states of the system, whereas the EXAFS, particularly with significantly high kinetic energies (to ~1000 eV above the E_o), can accurately determine the local structure or geometry.

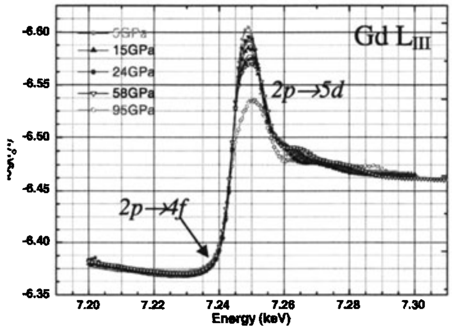

Figure 3. *The L_{III} XAS of compressed Gd, illustrating a continuous reduction of the 2p→4d transition intensity with pressure. The absorption spectra were obtained using two 0.5 mm-perforated diamond anvils to minimize the x-ray absorption.*

Figure 3 shows the L_{III} XAS of compressed Gd in the XANES region, consisting of a strong dipole allowed *2p→5d* transition in the near-edge (or, "white" line) and a weaker quadruple allowed *2p→4f* transition in the pre-edge region. The pressure-induced spectral change is most dominant in the near-edge region, showing a continuous decrease of the white-line intensity with an increase of pressure. Similar changes have been observed in the L_{III} XAS of Ce across the γ→α phase transition at low temperatures [10]. A plausible explanation of the pressure-induced white-line intensity decrease in both Ce and Gd is the *5d* (or, more generally, valence) electron hybridization with the *4f*. Such hybridization will induce fluctuation in *f*-electron valence and lead to a mixed valence ground state, as explained in Ce [10]. However, because of a significant *2p* core-hole broadening, the pre-edge feature of the L_{III} edge is unresolved in Fig. 3 and, as a result, the corresponding increase in the *4f* pre-edge intensity is not apparent. Nevertheless, as will be explained in the next section, the *4f-5d* hybridization becomes apparent in the M-edge x-ray absorption spectrum where the *4f* and the *5d* features are well resolved, as discussed in the next section.

B M-edge X-ray Absorption Spectra by Resonance Inelastic X-ray Scatterings

The M-edge absorption spectra can be resolved *via* inelastic x-ray scattering processes, utilizing high-energy (~7 KeV) incident x-ray near the L_{III} edge. Such experiments can be performed in two ways: (i) using x-ray resonance at the dipole-allowed transition – a relatively strong fluorescence process, referred to resonance x-ray emission spectroscopy (RXES) or (ii) using x-ray near the resonance – a weak inelastic Raman process which conserves both energy and momentum of the incoming x-ray and is often referred to resonance inelastic x-ray scattering (RIXS). The RXES provides the conduction electron DOS, identical to low-energy M-edge x-ray absorption spectra. The RIXS experiment, on the other hand, can be performed on a single crystal to obtain the pressure- and angular- dependences of *p,d,f*-electron orbitals near the Fermi level (within a few eV) – not demonstrated at high pressures.

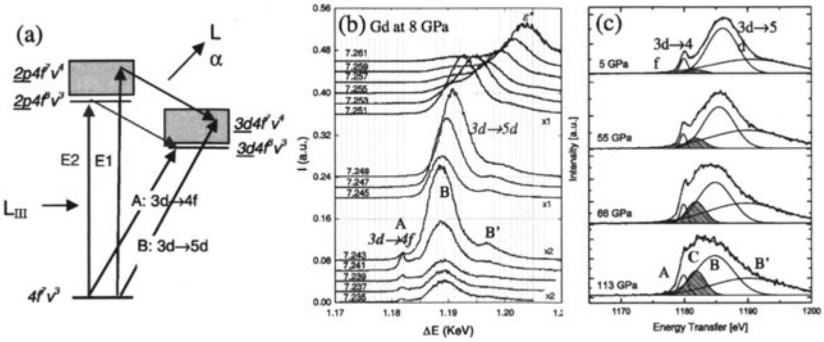

Figure 4 (a) A schematic illustrating the 2p3d RXES process in Gd, (b) the RXES at 8 GPa, plotted as a function of energy transfer ΔE between the incident x-ray energy Ω (marked on each spectra) and the fluorescence x-ray fluorescence ω, and (c) the pressure-induced change in Gd RXES at Ω= 7.241 KeV, showing a new feature C arising from the pressure-induced f-electron hybridization.

In the RXES experiments, we measure the Lα x-ray emission (ω) which corresponds to 2p ⟶ 3d core-hole decay at around 6.05 KeV, following high energy x-ray excitation near the L_{III} absorption edge (Ω) which corresponds to quadruple allowed E2: 2p ⟶ 4f transition at 7.241 keV and E1: dipole allowed 2p ⟶ 5d at 7.247 keV of Ga. Then, plotting the measured emission intensities as a function of the energy transfer ΔE = Ω – ω is the RXES that carries the same information of the M-edge x-ray absorption, as illustrated in Fig. 4(a).

The characteristic of the Gd RXES at 8 GPa (Fig. 4(b)) is analogous to those previously obtained from the Gd oxide [11] and consists of three main features: (i) a strong feature B at ΔE=1186 eV which resonates at Ω=7247 eV corresponding to the dipole-allowed E1: 2p → 5d transition, (ii) a substantially weaker peak A at 1180 eV, resonating at 7239 eV corresponding to the quadruple allowed E2: 2p → 4f transition, and (iii) a broader feature B' at <1191 eV with the same resonance characteristics as peak B. Incident energies above 7247 eV correspond to excitations into continuum states (ε^*), representing non-resonant XES.

At higher pressures, however, significant spectral changes occur in the RXES, as shown in Fig. 4(c). The most striking one is the new feature C at around 1182 eV, which rapidly increases the intensity with increasing pressures. This new feature can be understood in terms of the pressure-induced electron hybridization, resulting in the growth of the f^6v^4 and f^8v^2 components of the wave function at the expense of the predominant f^7v^3. Note that the *v* refers to valence electron in the *5d6s* orbitals in Fig. 4(a). Having such a mixed ground state, the peak C can be understood in terms of the transition from the f^8v^2 to the same final state multiplet of the A, f^8v^3 (or $3\underline{d}4f^8(5d6s)^3$), but *via* a dipole-allowed intermediate state f^9v^2, instead of a quadruple allowed f^7v^3 to f^8v^3 transition of the A. Therefore, the new feature C becomes progressively stronger with respect to the A or B peaks, as the pressure (or, the mixing ratio) increases. The splitting between the A and C peaks, ~2 eV, is then a measure of the *on-site* electron correlation of *f*-electrons in Gd. A quantitative spectral analysis of the RXES data yields that the mixed valence ratio increases exponentially with increasing density to around 0.2 at 100 GPa [6] - a value comparable to that of γ-Ce at the ambient pressure [12].

C Lγ X-ray Emission Spectroscopy (XES)

An important question regarding the correlation-driven transitions in *f*-electron metals is whether the local magnetic moment of *f*-electrons is quenched (*i.e.,* Mott transition) or screened out (Kondo-like models) in the itinerant phase. The existing experimental data is inconclusive in this aspect, even in the most extensively studied Ce at the ambient pressure. For example, the low temperature α(*fcc*)-Ce phase has long been thought of an itinerant phase, because of its weak temperature dependent magnetic susceptibility which suggests a Pauli paramagnet [13]. However, in recent years, there has been an increasing number of experimental evidences showing strong electron correlation in this phase [12,14].

The information regarding the local magnetic moment of *f*-electrons can be obtained by x-ray emission spectroscopy (XES) which probes the coupling between a core-hole and spin-localized electrons, as demonstrated in many lanthanide compounds and *3d*-magnetic transition metal monoxides (TMO) such as MnO [7] and Fe_2O_3 [15]. The electrostatic interactions between the *4d* (or *2p*) core-hole and the *4f* (or *3d*) electrons are so large in lanthanide compounds (or TMO) that give rise to well-separated satellite structures, as shown in Fig. 5. Therefore, the detailed satellite structure offers the information of the spin polarization; to a first approximation, the energy separation $\Delta E = J/(2S+1)$ and the branching ratio $I'/I = S/(S+1)$, where J and S are, respectively, the exchange integral and the spin angular momentum [16].

Important to note is that XES probes a core-hole-electron transition that occurs very fast (in ~fs) and, thus, provides a snap shot of the local moment in both para- and ferromagnetic materials. Therefore, XES is capable of probing the local *f*-electron moment even under a dynamically screened situation, so as to reveal if the expected Pauli-like susceptibility is originated from quenched or simply screened out *f*-electron moments at high pressures. In this regard, the XES experiments complement the magnetic susceptibility and x-ray circular dichroism measurements, both of which measure a slow process of spin polarization and thus largely an ordered moment in ferromagnetic solids.

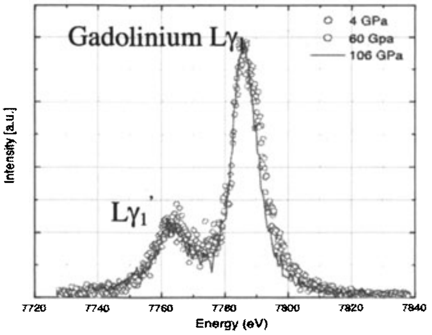

***Figure 5**. $L\gamma_1$ XES of Gd at 4, 65, and 106 GPa, normalized to the main peak intensity, showing no apparent change in the $L\gamma'_1$ satellite peak intensity, suggesting no changes in the 4f moments up to 106 GPa.*

Figure 5 shows the $L\gamma_1$ XES in Gd, corresponding to the core-hole decay from the 2p → 4d, at high pressures. Clearly, the pressure dependence shows no apparent change in the XES spectra and thus no local moment change in Gd to 106 GPa-well beyond the volume collapse transition ~60 GPa. This behavior of XES in Gd is in contrast to nearly complete loss of 3d moments of Mn and Fe in TMO across the Mott transition [7,14], but is consistent with the observed *f*-electron hybridization in Gd as well as Ce [12,14].

SUMMARY

The present XAS, both the L_{III} and M_{III}-edges of Gd suggests significant *f*-electron delocalization to occur at high pressures which causes increasing fluctuations away from the sharp f^7 character of the localized limit. The degree of hybridization can be quantitatively probed by RXES even at pressures over 100 GPa, suggesting that the *f*-electrons of the high-pressure Gd phases (well above the volume collapse transition) are still highly correlated. This result is, in turn, consistent with the recent experimental evidence of strong electron correlation in the α-Ce phase [12,14]. As seen here for f^7 Gd, this process is prolonged and continuous as a function of volume. This suggests that the volume collapse transition is only part of the phenomenon and acts to accelerate the delocalization. The present XES results suggest that the bare *4f* moment persists across the collapse transition in Gd so that any loss of temperature dependence in the magnetic susceptibility must then arise from Kondo-like screening of the moments.

The present study shows that a combined information of various synchrotron x-ray spectroscopies offers new ways to study electronic phase transitions in *f*-electron metals at high pressures. The example was shown in rare-earth metals, specifically Gd, yet the methods applied/developed in this study is equally well suitable for high-pressure studies of actinides, of which no electronic data is available and future studies should emphasize.

ACKNOWLEDGEMENT

The present study has been largely based on the data published in Ref. 6 and the work performed in collaboration with Drs. Andy McMahan at LLNL and Profs. R. Scalletar and W. Pickett at UCD, and Drs. M. Hu and P. Chow at HPCAT. The x-ray data were obtained at the HPCAT facility, supported by DOE-BES, DOE-NNSA (CDAC, LLNL, UNLV), NSF, and the W. M. Keck Foundation. The work at WSU has been supported by DOE-NNSA #DE-F603-97SF21388.

REFERENCES

1 A. McMahan, C. Huscroft, R.T. Scalettar, and E.L. Pollock, *J. of Computer-Aided Materials Design* **5**, 131 (1998).

2 S. Hecker, *Plutonium and its alloys from atoms to microstructure* in *Los Alamos Science*, November 26, (2000), p. 290.

3 B. Johansson, *Phys. Rev. B* **11**, 2740 (1975).

4 P. W. Anderson, *Phys. Rev.* **124**, 41 (1961).

5 J. W. Allen and R. M. Martin, *Phys. Rev. Lett.* **49**, 1106 (1982).

6 B. R. Maddox, A. Lazicki, C. S. Yoo, V. Iota, M. Chen, A. K. McMahan, M. Hu, P. Chow, R. T. Scalettar, and W. E. Pickett, *Phys. Rev. Lett.*, **96**, 215701 (2006).

7 C. S. Yoo, B. Maddox, J. H. P. Klepeis, V. Iota, W. Evans, A. McMahan, M. Hu, P. Chow, M. Somayazulu, D. Häusermann, R. T. Scalettar, and W. E. Pickett, *Phys. Rev. Lett.* **94**, 115502 (2005).

8 V. Iota, J.-H. Klepeis, C. S. Yoo, J. Lang, D. Haskel, and G. Srajer, *Appl. Phys. Lett.* **90**, 042505 (2007).

9 J. F. Lin, A. G. Gavrilliuk, V.V. Struzhkin, S.D. Jacobsen, W. Sturhahn, M.Y. Hu, P. Chow, and C. S. Yoo, *Phys. Rev. B* **73**, 11307 (2006).

10 C. Derella, M. Grioni, A. Palenzona, M. Taguchi, E. Annese, G. Ghiringhelli, A. Tagliaferri, N.B. Brookes, Th. Neisius, and L. Braicovich, *Phys. Rev. B* **70**, 085112 (2004).

11 M. Krisch, C.C. Kao, P. Sette, W.A. Caliebe, K. Hämäläinen, and J. B. Hastings, *Phys. Rev. Lett.* **24**, 4931 (1995).

12 J.-P. Rueff, C.F. Hague, J.-M. Mariot, L. Journel, R. Delaunay, J.-P. Kappler, G. Schmerber, A. Derory, N. Jaouen, and G. Krill, *Phys. Rev. Lett.* **93**, 067402 (2004).

13 M.R. MacPherson, G.E. Everett, D. Wohllenben, and M.B. Maple, *Phys. Rev. Lett.* **26**, 20 (1971).

14 A. P. Murani, S. J. Levelt, and J. W. Taylor, *Phys. Rev. Lett.* **95**, 256403 (2005).

15 J. Badro and G. Figuet, *Phys. Rev. Lett.* **89**, 20554 (2002).

16 F. de Groot, *Chem. Rev.* **101**, 1779 (2001).